Proceedings of the 10th World Congress on Mechanical, Chemical, and Material Engineering (MCM'24)
Barcelona, Spain –August 22-24, 2024
Paper No. HTFF 183
DOI: 10.11159/htff24.183

Numerical Investigation of Distance between Fan and Coil Block in a Fin and Tube Heat Exchanger

Harun Denizli[1], Mustafa Zabun[1], Feyza Şahin[1]
[1]Friterm A.S.
Istanbul Deri Organize Sanayi Bolgesi Dilek Sokak No: 10 X-12 Ozel Parsel Tuzla 34957 Istanbul / Türkiye
harundenizli@friterm.com; mustafazabun@friterm.com; feyzacebi@friterm.com;

Abstract **-** Heat exchangers are devices that are widely used to transfer heat between fluids due to their temperature differences. As a type of heat exchanger, oil coolers are heat exchangers that cool the oil as the air passes through the fins of heat exchanger by transferring heat from the oil to the air passes through the heat exchanger.

An assembled fin and tube heat exchanger consists of a coil block and a casing with a fan mounted on it. The term “Fan hood” is used to define the distance between the fan and the coil block. Oil coolers play a crucial role in cooling systems, and their heat transfer performance can vary depending on design parameters. These parameters can be related to the air side or the internal fluid side. For air side efficiency, the distance between the fan and the coil block effects the performance by creating dead zones at the corners of the casing and maldistribution of air flow. Therefore, a detailed study of the effect of the fan hood on the heat exchanger and the optimum fan hood distance is necessary for an efficient oil cooler design.

This study aims to investigate the value of the fan hood in a fin and tube type oil cooler heat exchanger through computational fluid dynamics (CFD) simulations and experimental investigations. CFD simulations will be used to study the air flow within the fan hood. These simulations will provide valuable insights to optimise the design of the fan hood. In addition, experimental tests will be carried out to validate the CFD results and to measure the performance of the fan hood under real conditions.

The results will help us to understand the effect of fan hood design on heat exchanger efficiency and contribute to the development of more efficient cooling systems. This study will provide essential information for heat exchanger design and improving the energy efficiency of cooling systems.

***Keywords*:** Fan hood, fin and tube air cooler, heat exchanger, numeric analysis, CFD

1. Introduction

Heat exchangers are indispensable devices utilized across various industries to facilitate the transfer of heat between fluids, exploiting temperature differentials for efficient thermal management[1]. Among the diverse array of heat exchangers, oil coolers stand out as critical components, tasked with cooling oil by exchanging heat with the surrounding air as it passes through the fins of the heat exchanger.

Comprising a coil block and a casing housing a fan, assembled fin and tube heat exchangers play a pivotal role in cooling systems. The term "Fan hood" denotes the distance between the fan and the coil block, a parameter of paramount importance for optimizing heat transfer efficiency. In the context of oil coolers, the effectiveness of heat transfer is contingent upon meticulous consideration of design parameters, both on the air side and within the internal fluid circuit.

Of particular significance to air side efficiency is the spacing between the fan and the coil block, as it influences airflow distribution and may lead to the formation of dead zones within the casing, thereby compromising performance. Hence, a comprehensive examination of the impact of the fan hood on heat exchanger efficiency, coupled with the determination of the optimal fan hood distance, is imperative to ensure the efficacy of oil cooler designs.

In finned tube heat exchangers, different features are considered together for the optimum selection of design parameters. It is aimed to design the most efficient product both on the air side and on the fluid side with low cost. Efficient product design on the air side depends on design features such as proper selection of design gaps, selection of fin properties to provide appropriate pressure loss.

In the literature, numerical and experimental studies on different fin types have been carried out and the effect of lamella types on performance has been investigated. The studies have been carried out mostly with bare coils, and fewer studies have been carried out on fan-mounted products.

Altwieb et al. introduced new geometric designs for a multi-tube, multi-fin heat exchanger, focusing on three different configurations: plain, perforated plain, and louvered fin heat exchangers. The experiments revealed that louvered fins consistently provided the highest heat transfer rates across various air and water flow rates[2].Sibtain et al. conducted a numerical simulation to analyse the efficiency of a counter-flow shell and tube heat exchanger, both with and without inner fin geometry[3].Jabardo et al. investigated the air side performance of herringbone-wavy and convex-louver fin coils. They found Colburn and friction factors are not significantly affected by tube rows in multi-row wavy and louver fin coils, while they vary notably in single-row wavy coils[4].Liu et al. enhances the heat transfer efficiency of a standard herringbone wavy fin-tube heat exchanger by optimizing the wavy fin geometries and perforation parameters[5].

2. Model Description

The effect of the distance between the fan hood and the heat exchanger on pressure loss will be examined. Improving this parameter is of great importance for manufacturers. While a greater distance may be beneficial for flow, it results in additional costs for the manufacturer.

Experimental studies will first be conducted on a product when investigating this parameter. Validation of numerical data will be conducted using the results obtained from these experiments. After validation, parametric research will be carried out to optimize the gap between the fan hood and the fins.

2.1. Experimental Setup

The experimental model was designed to determine the pressure loss of the heat exchanger at different air velocities. Accordingly, it was decided to use a heat exchanger called a dry cooler designed with an EC fan capable of operating at different speeds. The specifications of the heat exchanger designed for the test are given in Table 1.

Table 1: Specification of the dry cooler heat exchanger

Geometry	F3833	Number of Circuits	30
Tube Diameter (mm)	15	Finned Length (mm)	1400
Tube Material	Copper	Fin Thickness (mm)	0,12
Number of Tube	30	Fin Material - Type	Aluminium - Corrugated
Number of Row	4	Number of Circuits	30

The pressure loss of this heat exchanger will be measured with a differential pressure sensor. The differential pressure sensor is a measurement device that provides the static pressure loss between two points. One input of this device will be placed at the air inlet of the product, and the other input will be placed between the heat fins and the fan.

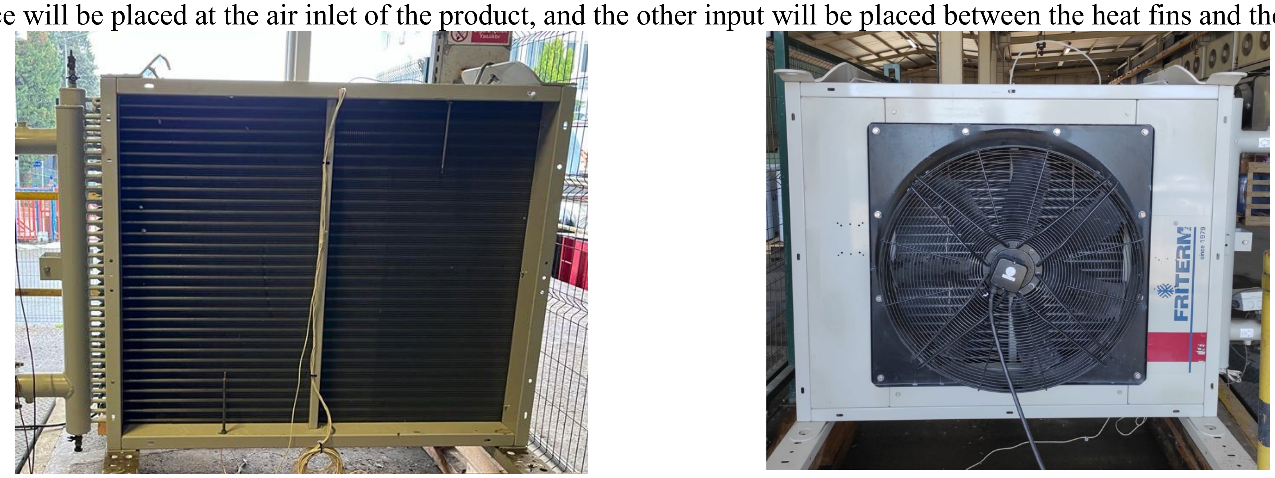

Fig. 1: The heat exchanger to be tested

To obtain a more precise measurement, data will be collected from the pressure sensor placed between the fins and the fan at several points.

The general technical information of the differential pressure sensor device is provided in the table below.

Table 2: General Information of the Differential Pressure Sensor

Range	-15 kPa to 15 kPa
Accuracy	±5 Pa (0…100 Pa) ±(2 Pa + %1.5 of the measured value) (100 … 15,000 Pa)
Resolution	1 Pa
Operating Temperature	-20…+50 °C

The difference between the average of the pressures taken from a total of three points, including two points from the right and left sides of the product and one point from the top, and the inlet pressure is measured.

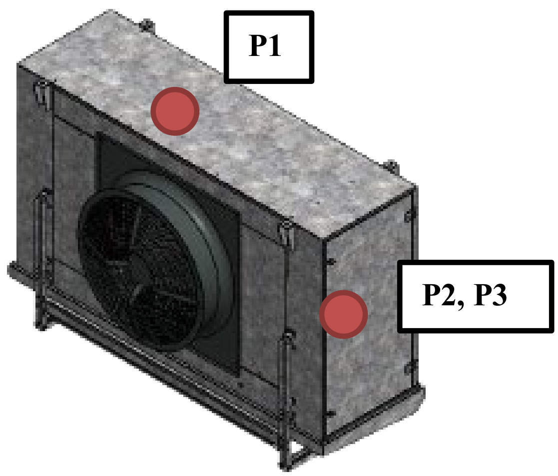

Fig. 2: Measurement points of static pressure

After determining these measurement points, the speed of the EC fan will be controlled using a potentiometer to record the pressure losses it produces at different air velocities.

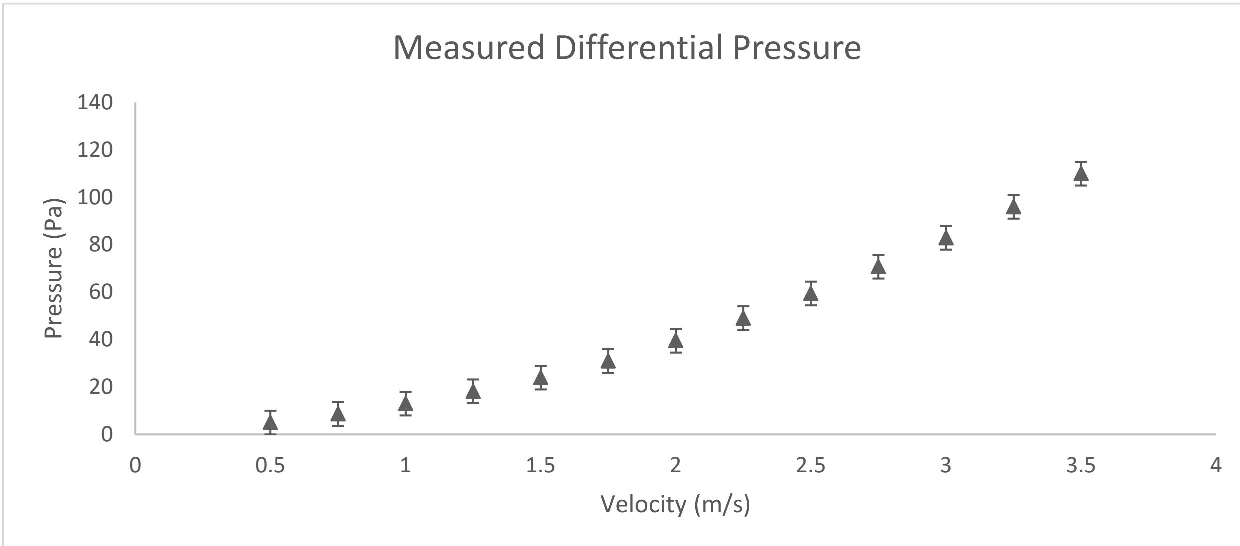

Fig. 3: Air side pressure loss values measured from the heat exchanger

2.2. Numerical Model

It was decided to create a porous media in that region when constructing the numerical model to determine the pressure losses of the fins in the product. This porous media will simulate the pressure loss on the fin. In this analysis, it was considered that there is no need for three dimensions because the product progresses symmetrically from top to bottom. Therefore, the analysis will be conducted in two dimensions. In the two-dimensional analysis, the product will be designed based on the top view. When viewed from the top, the product will have the following components from the air inlet to the outlet (Figure 4):

1. Air inlet
2. Coil (Fin and tube)
3. Fan Hood
4. Fan

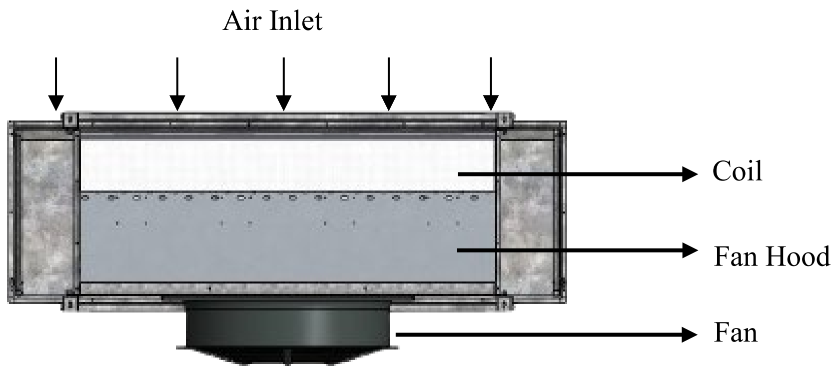

Fig. 4: Basic definition of the dry cooler heat exchanger

The conceptual design of the analysis is provided in Figure 5. Air will enter from region 1 and exit from region 3. The other regions will be defined as walls.

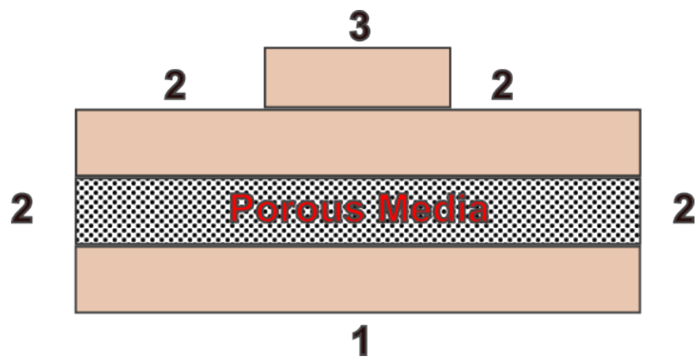

Fig. 5: Illustration of the CFD model

The boundary condition indicated by number 1 is the Velocity Inlet, the boundary condition indicated by number 2 is Wall, and the boundary condition indicated by number 3 is Pressure Outlet.

2.2.1. Mesh Independence

A mesh independence analysis is a technique used to determine if the simulation outcomes remain consistent regardless of the mesh structure. This is achieved by conducting multiple simulations with varying mesh resolutions to assess any fluctuations in the results. Such an inquiry is pivotal in computational fluid dynamics (CFD) due to the intricacies of CFD simulations and the foundational mathematics involved.

By altering the element size, variations in the pressure loss values will be observed under the same conditions.

Table 3: Pressure dependence by changing mesh element size

Case No	Element Size (mm)	Mesh Elements	Pressure Drop (Pa)
1	10	7288	38,82
2	5	28708	39,02
3	2	180790	39,578
4	1	713326	39,588
5	0,5	3002478	39,601

As can also be seen from the table, the change in pressure loss based on the number of meshes after Case 3 is lower compared to the other cases. Therefore, the number of elements in Case 3 will be used.

2.2.2. Verification of the Numerical Model

To validate the numerical model, the product will be drawn and analysed in two dimensions. The lengths of the drawn geometry are provided as follows.

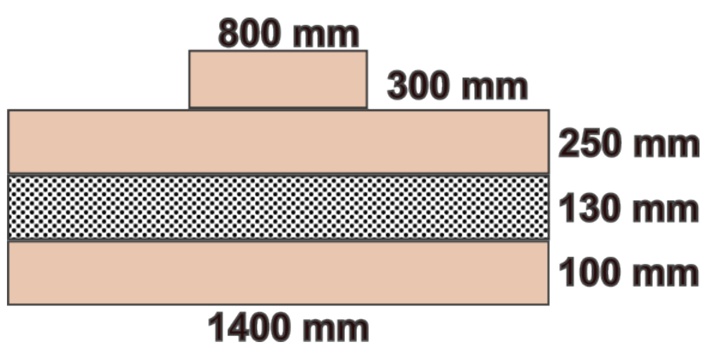

Fig. 6: Dimensions of the numerical model

In this model, pressure loss values will be obtained for 5 different velocities: 1.5, 2, 2.5, 3, and 3.5 m/s, and compared with experimental data.

Table 4: Comparison of the numerical and experimental results

Velocity (m/s)	Experimental Data (Pa)	Numerical Data (Pa)	Error (%)
1,5	23,96	23,35	2,55%
2	39,5	39,76	0,66%
2,5	59,43	60,48	1,77%
3	82,92	85,52	3,14%
3,5	109,95	114,87	4,47%

As seen here, the errors are less than 5%. A margin of error of up to 15% is allowed in the numerical modeling. Therefore, this model can be used for this case.

2.3. Mathematical Model

The governing system of equations can be written as follows:

Continuity equation:

$$\frac{\partial \rho}{\partial t} = -\nabla \cdot (\rho\, \mathbf{V}) \tag{1}$$

Where, V: velocity, ρ: Density

Momentum equation:

$$\left(\frac{\partial(\rho u)}{\partial t} + \nabla(\rho \mathbf{u}\mathbf{V})\right) = -\frac{\partial P}{\partial x} + \rho \boldsymbol{F}_{\boldsymbol{x,body}} + \boldsymbol{F}_{\boldsymbol{x,viscous}} \tag{2}$$

Where, P: Pressure, F: Force

Porous media are simulated by incorporating a momentum source term into the conventional fluid flow equations. This source term consists of two components: a term for viscous losses and a term for inertial losses.

$$S_i = \sum_{j=1}^{3} \boldsymbol{D_{ij}} \mu \boldsymbol{v_j} + \sum_{j=1}^{3} \boldsymbol{C_{ij}} \frac{\mathbf{1}}{\mathbf{2}} \boldsymbol{\rho} |\boldsymbol{v}| \boldsymbol{v_j} \tag{3}$$

where:

S_i :Source term for the i_{th}(x, y or z) momentum equation, D and C: Prescribed matrices

3. Simulation Results

In numerical analysis, in order to compare the parameter results, a dimensionless ratio will be defined to scale the fan hood distance. This ratio is defined as follows:

$$\eta = \tan\alpha = \frac{X_{FH}}{X_L}$$

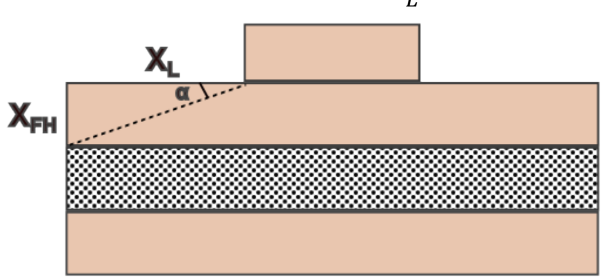

Fig. 7: Definition of the ratio

A parametric study was conducted to optimize the length of the section between the fan and the fins. Several parameters will be determined in Table 5.

Table 5: Parameters for the numeric analysis

Case No	Ratio	Velocity (m/s)	Finned Length (mm)	Fan Hood Length (mm)	Fan Diameter (mm)
001…015	0,25	1,2,3	1400,1600,1800,2000,2200	75	800
016…030	0,5	1,2,3	1400,1600,1800,2000,2200	150	800
031…045	0,75	1,2,3	1400,1600,1800,2000,2200	225	800
046…060	1	1,2,3	1400,1600,1800,2000,2200	300	800
061…075	1,25	1,2,3	1400,1600,1800,2000,2200	375	800
076…090	1,5	1,2,3	1400,1600,1800,2000,2200	450	800
091…105	1,75	1,2,3	1400,1600,1800,2000,2200	525	800
106…120	2	1,2,3	1400,1600,1800,2000,2200	600	800

The numerical analyses were conducted for the aforementioned cases, and the results are provided in the tables below. The tables also include the percentage improvements in pressure loss for the case with the smallest length.

Table 6: Results of the numeric analysis

Finned Length :1400 mm							
Hood Length (mm)	η	1 m/s		2 m/s		3 m/s	
		Pressure Drop (Pa)	Pressure Loss Improvement(%)	Pressure Drop (Pa)	Pressure Loss Improvement(%)	Pressure Drop (Pa)	Pressure Loss Improvement(%)
75	0,25	13,839	0,00%	49,863	0,00%	108,080	0,00%
150	0,50	12,122	12,41%	43,169	13,42%	93,137	13,83%
225	0,75	11,405	17,59%	40,357	19,06%	86,853	19,64%
300	1,00	11,022	20,36%	38,865	22,06%	83,534	22,71%
375	1,25	10,780	22,10%	37,929	23,93%	81,474	24,62%
450	1,50	10,605	23,37%	37,277	25,24%	80,053	25,93%
525	1,75	10,488	24,21%	36,859	26,08%	79,093	26,82%
600	2,00	10,400	24,85%	36,595	26,61%	78,496	27,37%
Finned Length: 1600 mm							
Hood Length (mm)	η	1 m/s		2 m/s		3 m/s	
		Pressure Drop (Pa)	Pressure Loss Improvement(%)	Pressure Drop (Pa)	Pressure Loss Improvement(%)	Pressure Drop (Pa)	Pressure Loss Improvement(%)
100	0,25	16,164	0,00%	59,125	0,00%	128,9	0,00%
200	0,50	13,733	15,04%	49,612	16,09%	107,63	16,50%
300	0,75	12,806	20,77%	45,97	22,25%	99,486	22,82%
400	1,00	12,338	23,67%	44,14	25,34%	95,411	25,98%
500	1,25	12,055	25,42%	43,029	27,22%	92,963	27,88%
600	1,50	11,855	26,66%	42,259	28,53%	91,331	29,15%
700	1,75	11,729	27,44%	41,827	29,26%	90,385	29,88%
800	2,00	11,664	27,84%	41,499	29,81%	89,588	30,50%
Finned Length: 1800 mm							
		1 m/s		2 m/s		3 m/s	

Hood Length (mm)	η	Pressure Drop (Pa)	Pressure Loss Improvement(%)	Pressure Drop (Pa)	Pressure Loss Improvement(%)	Pressure Drop (Pa)	Pressure Loss Improvement(%)
125	0,25	18,547	0,00%	68,634	0,00%	150,28	0,00%
250	0,50	15,441	16,75%	56,449	17,75%	123,03	18,13%
375	0,75	14,341	22,68%	52,115	24,07%	113,32	24,59%
500	1,00	13,805	25,57%	50,015	27,13%	108,64	27,71%
625	1,25	13,491	27,26%	48,772	28,94%	105,83	29,58%
750	1,50	13,279	28,40%	47,914	30,19%	104,08	30,74%
875	1,75	13,186	28,90%	47,498	30,80%	103,14	31,37%
1000	2,00	13,179	28,94%	47,157	31,29%	102,44	31,83%
Finned Length: 2000 mm							
Hood Length (mm)	η	1 m/s		2 m/s		3 m/s	
		Pressure Drop (Pa)	Pressure Loss Improvement(%)	Pressure Drop (Pa)	Pressure Loss Improvement(%)	Pressure Drop (Pa)	Pressure Loss Improvement(%)
150	0,25	21,002	0,00%	78,452	0,00%	172,36	0,00%
300	0,50	17,277	17,74%	63,804	18,67%	139,59	19,01%
450	0,75	16,025	23,70%	58,866	24,97%	128,52	25,44%
600	1,00	15,437	26,50%	56,546	27,92%	123,33	28,45%
750	1,25	15,078	28,21%	55,203	29,63%	120,3	30,20%
900	1,50	14,908	29,02%	54,417	30,64%	118,5	31,25%
1050	1,75	14,769	29,68%	53,81	31,41%	117,23	31,99%
1200	2,00	14,708	29,97%	53,613	31,66%	116,92	32,17%
Finned Length: 2200 mm							
Hood Length (mm)	η	1 m/s		2 m/s		3 m/s	
		Pressure Drop (Pa)	Pressure Loss Improvement(%)	Pressure Drop (Pa)	Pressure Loss Improvement(%)	Pressure Drop (Pa)	Pressure Loss Improvement(%)
175	0,25	23,557	0,00%	88,668	0,00%	195,36	0,00%
350	0,50	19,245	18,30%	71,69	19,15%	157,34	19,46%
525	0,75	17,866	24,16%	66,25	25,28%	145,13	25,71%
700	1,00	17,225	26,88%	63,715	28,14%	139,48	28,60%
875	1,25	16,863	28,42%	62,28	29,76%	136,25	30,26%
1050	1,50	16,728	28,99%	61,729	30,38%	134,89	30,95%
1225	1,75	16,607	29,50%	61,221	30,95%	133,56	31,63%
1400	2,00	16,458	30,14%	60,576	31,68%	132,31	32,27%

4. Conclusion

Upon examination of the numerical analysis results, the following conclusions have been reached:

For different velocities: When the hood length increases at different velocities, it is observed that there is no change in the improvements.

For different finned length values: As the fin length value increases, along with the increase in pressure loss, the percentage of improvement also increases as the fan hood length increases. Therefore, in products where the fin length per fan is high, more attention should be paid to the fan hood length.

When examining the required fan hood length in heat exchangers, the percentage of pressure loss improvement is found to stabilize at approximately 1 where the specified ratio is 1. Since it is important for heat exchanger manufacturers to keep this length as small as possible for product efficiency, it is crucial that this ratio does not fall below 0.75 for product efficiency. This actually leads to the conclusion that the ideal angle should be 45 degrees as stated, and it should be a minimum of 37 degrees.

Acknowledgements

We would like to express our gratitude to Friterm, the company we work for, for their permission to use the products and measurement tools in this study, as well as for their support towards academic research. Additionally, we extend our thanks to Professor Dr. Feridun Ozguc for his assistance in this study.

References

[1] ETSU, “Compact Heat Exchangers - Guidance for Engineers.” p. 255, 2000.

[2] M. Altwieb, R. Mishra, A. M. Aliyu, and K. J. Kubiak, “Heat Transfer Enhancement by Perforated and Louvred Fin Heat Exchangers,” *Energies*, vol. 15, no. 2, 2022, doi: 10.3390/en15020400.

[3] M. Sibtain, H. Liang, M. R. Uddin, M. A. Mond, A. A. Ansari, and M. Z. U. Khan, “Investigating the Heat Transfer Characteristics of Fin-prolonged Heat Exchanger for Waste Heat Recovery,” *2023 14th Int. Conf. Mech. Intell. Manuf. Technol. ICMIMT 2023*, pp. 234–237, 2023, doi: 10.1109/ICMIMT59138.2023.10201099.

[4] J. M. Saiz Jabardo, J. R. Bastos Zoghbi Filho, and A. Salamanca, “Experimental study of the air side performance of louver and wave fin-and-tube coils,” *Exp. Therm. Fluid Sci.*, vol. 30, no. 7, pp. 621–631, 2006, doi: 10.1016/j.expthermflusci.2006.01.001.

[5] X. Liu, M. Wang, H. Liu, W. Chen, and S. Qian, “Numerical analysis on heat transfer enhancement of wavy fin-tube heat exchangers for air-conditioning applications,” *Appl. Therm. Eng.*, vol. 199, no. May, p. 117597, 2021, doi: 10.1016/j.applthermaleng.2021.117597.